JOURNAL OF OPTOELECTRONICS AND ADVANCED MATERIALS Vol. 10, No. 5, May 2008, p. 1011-1016

On the magnetic resistance of YBaCuO bulk superconductor dynamically interacting with perturbed flux of iron-homopolar magnetic track

G. D'OVIDIO*, F. CRISI, G. LANZARA
Transportation Dept DAU, Faculty of Engineering, University of L'Aquila, 67040 - Monteluco di Roio, Italy

This article deals with the magnetic resistance that arises in the cooled high temperature superconductor (HTS) bulk, dynamically interacting with a frequently perturbed flux of magnetic track employing homopolar permanent magnets (PM) arranged within an "U" shaped loose iron core. The influence of flux perturbation on the magneto-dynamic maglev performance of HTS bulk is studied and tested by means of an experimental ring model device employing the same passive YBaCuO structure interacting with a magnetic track field differently perturbed by several iron plates radially and frequently distributed on the circular track. This experimental model device reproduces, by analogy, the magneto-dynamic behavior of a vehicle with HTS onboard riding above an uneven magnetic guideway. Finally, magnetic resistances and lift forces have been tested and the results are compared and discussed.

(Received March 13, 2008; accepted May 5, 2008)

Keywords: Magnetic levitation, YBaCuO bulk superconductor, Permanent magnets, Transportation application

1. Introduction

The levitation performance of a YBaCuO bulk superconductor, because of its inherent stability, is an important applications characteristic for use in a perfect magnetically levitated (maglev) transportation systems [1], [2].

It is well known that for a one dimensional system the levitation force behavior is influenced by the critical current density J_C, the geometrical characteristics of YBaCuO (dimension, shape, thickness), magnetic field gradient *dH/dz*, cooling process, operating temperature, and so on.

At the University of L'Aquila, a novel technological demonstrator of a scaled maglev HTS vehicle driven by a DC linear motor riding on a guideway section with permanent magnets has been already designed and manufactured.

To define the system configuration, propaedeutical experiences on magnetic suspension, guidance and propulsion have already been acquired by using an experimental model device using the same passive YBaCuO secondary ring interacting with different circular primaries (tracks) that generate the following magnetic field typologies:

a) Translating by windings three-phase voltage fed;
b) Static and alternating by PM in Halbach array;
c) Static and uniform by iron-homopolar PM.

The first the system combines lift and propulsion forces [3], the second system produces both lift and drag forces [4] and the third system generates lift force only [5].

In this paper we investigate the magnetic resistance in the cooled YBaCuO bulk, dynamically interacting with a perturbed field generated by an iron-homopolar magnetic guideway.

Three configurations of the guideway with different magnetic characteristics have been designed, manufactured, and replaced in the experimental device.

The experiments include three groups, the first group was carried out by YBaCuO ring dynamically interacting with a constant and uniform magnetic field of circular iron-magnetic track; the second and third groups of experiments were performed by starting from this primary configuration and by adding several iron plates in such a way to create two different types of flux disturbers. Finally, the experimental results are compared and discussed.

2. Experimental set-up

An experimental set-up reproducing the magneto-dynamic interaction between HTS and the different types of magnetic field was designed and manufactured.

The device (Fig. 1) consists of two main components with no physical contact between them:

1) *Secondary*: an HTS passive ring (Fig. 2) constituted by a close array of 34 YBaCuO trapezoidal shaped monoliths properly fitted on the bottom of the circular vessel filled with liquid nitrogen; the main design data of the YBaCuO ring are listed in Table 1;

Table 1. Design data of YBaCuO ring.

Outer radius	176.6	mm
Inner radius	217.5	mm
Average radius	196.6	mm
Thickness	11	mm
Trapped field	> 1	T (77K)
Critical current density	$> 8 \cdot 10^4$	A/cm^2 (77K, self field)

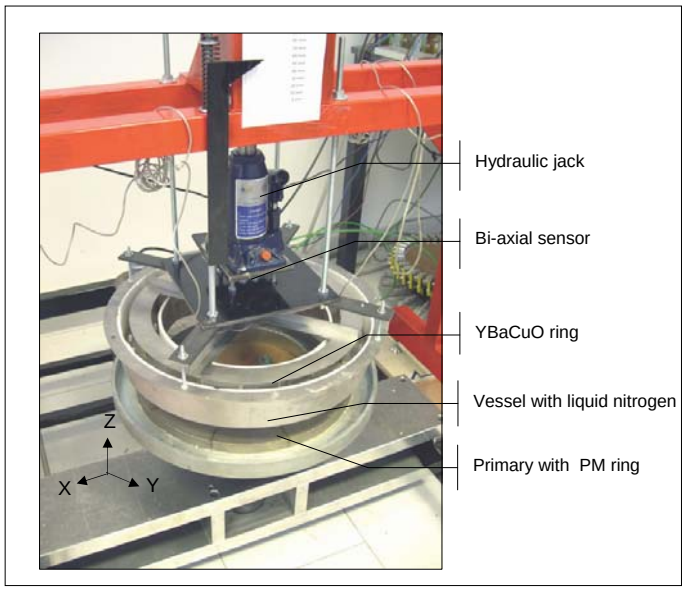

Fig. 1 Ring model device overview.

2) *Primary*: iron-magnetic circular inductor (Fig. 3), with the same average radius (197 mm) as the secondary one, composed by a homopolar Nd-Fe-B permanent magnet ring axially polarized and fixed on the middle crown of a loose "U" shaped iron structure. Table 2 lists the main design data of primary. This primary generates constant and uniform flux distribution along the annular direction. Starting from this configuration, two other primaries have been obtained by adding 6 and 12 rectangular iron plates (150×25×7mm) respectively, radially and equally distributed on the top side of track according to the illustrations shown in Fig. 4 and Fig. 5. In other terms, by adding iron plates we create more flux perturbation.

Table 2. Main data of circular inductor.

Iron ring	Outer radius	261.6	mm
	Inner radius	131.6	mm
	Average radius	196.6	mm
PM Ring	Outer radius	216.6	mm
	Inner radius	176.6	mm
	Average radius	196.6	mm
	Thickness	25	mm

Fig. 2. YBaCuO ring.

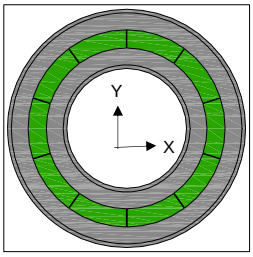

Fig. 3. Primary scheme with k=0

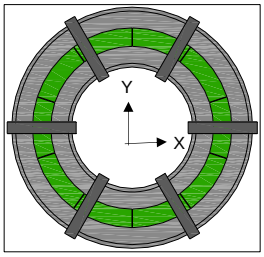

Fig. 4. Primary scheme with k=0.14.

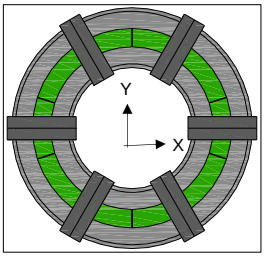

Fig. 5. Primary scheme with k=0.33.

In the experimental set up, the circular track and YBaCuO ring are mounted on a mechanical precision device in such a way that the air-gap can be varied (Fig. 1) The primary can rotate around its vertical shaft that is coupled to the a.c. motor fed with an inverter to reproduce wide work and slip conditions.

The interaction forces are tested on the secondary by a measurement system consisting of a torque (drag force) and thrust (lift force) bi-axial sensor.

Compared to the HTS maglev vehicle riding above the magnetic guideway, this ring device creates the following analogies:

(a) The primary simulates the magnetic way;

(b) The secondary simulates the superconducting "runner" onboard the vehicle;

(c) The relative motion is obtained by locking the secondary and imposing mechanical rotation of the primary.

2. Results and discussion

All of the tests have been performed following the steps stated below:

1. Measurements of magnetic flux perturbation;
2. Tests of levitation (lift and drag forces)

2.1 Flux measurements

Firstly the uniform and perturbed magnetic flux generated by different types of primaries have been measured on the middle crown of annular direction.

We define a flux perturbation factor k as the ratio between total iron plates top surface and PM ring top surface (50775 mm^2).

Consequently three different primary configuration with k=0 (unperturbed), k=0.14 (perturbed) and k=0.33 (strongly perturbed) are obtained.

Fig. 6 shows, for k=0 and k=0.14, the comparison of flux density Vs. annular abscissa of primary at different air-gaps and 0 rpm. As it is pictured in the cross section scheme shown in Fig. 6, the radial axis of iron plate corresponds to 0 annular abscissa of primary. We can see that at k=0 the flux configuration (dashed curves) is uniform and so unperturbed. On the contrary, at k=0.14 the flux configuration (continuous curves) is warped by the presence of iron plates according to the gap decrease; in correspondence to the lowest gap, the iron plate causes the breaks in continuity of flux since the plate shunts all the magnetic flux.

The magnitude of flux perturbation is inversely proportional to the size of the air-gap.

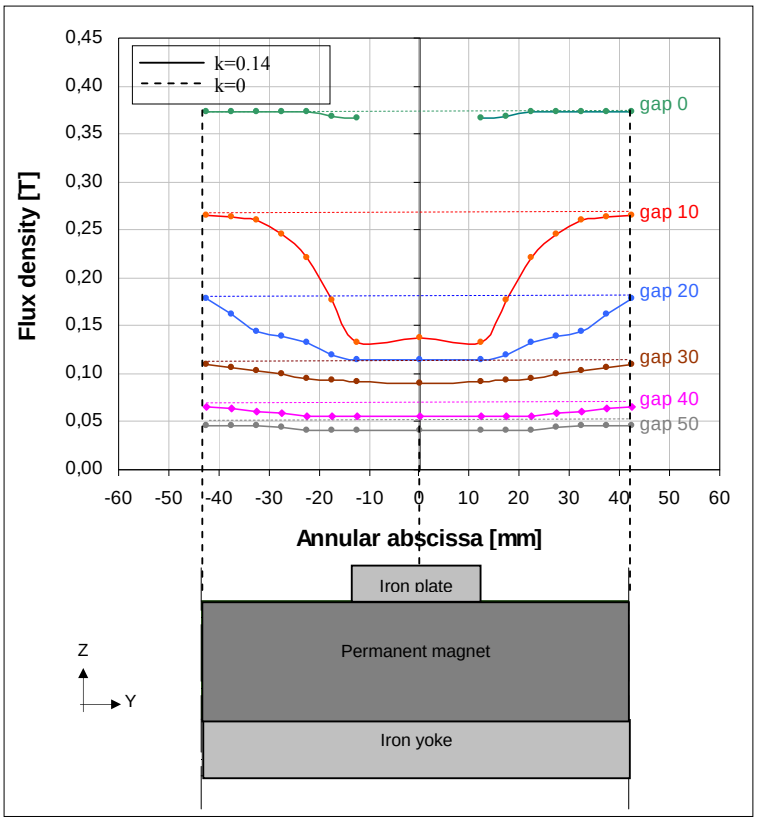

Fig. 6. Flux density Vs. annular abscissa for different gaps at k=0 and k=0.14 (0 rpm).

2.2 Levitation tests

Secondly, the levitation tests were performed at a track rotational speed of 150 rpm by cooling the YBaCuO in a zero magnetic field with liquid nitrogen.

The experiments include three groups carried out by the interaction of the cooled YBaCuO ring with the following magnetic flux types:

1. uniform (k=0);
2. perturbed (k=0.14);
3. strongly perturbed (k=0.33).

To compare the results of the tests, we define specific lift force (P_Z) and specific drag force (P_Y), as indicated in the following relations:

$$P_Z=F_Z/S_R \quad (N/cm^2) \tag{1}$$

$$P_Y=F_Y/S_R \quad (N/cm^2) \tag{2}$$

where F_Z and F_Y are lift and drag forces respectively and S_R (49370 mm^2) is the induced YBaCuO ring surface.

The entity of drag force (F_Y) is obtained by dividing the measured torque value by the average radius (0.1966m) of YBaCuO ring.

Fig. 7 shows P_Z and P_Y Vs. air-gap in correspondence of uniform flux (k=0) at a track rotational speed of 150 rpm. One can see that the no specific drag force P_Y is generated at every air-gap sizes while the specific lift force P_Z is inversely proportional to the size of the air-gap.

It has fully been verified and tested that this system configuration operates with a large air-gap and no feedback control for stable levitation is required [5]: these peculiarities are perfectly suitable to applications for the transportation system.

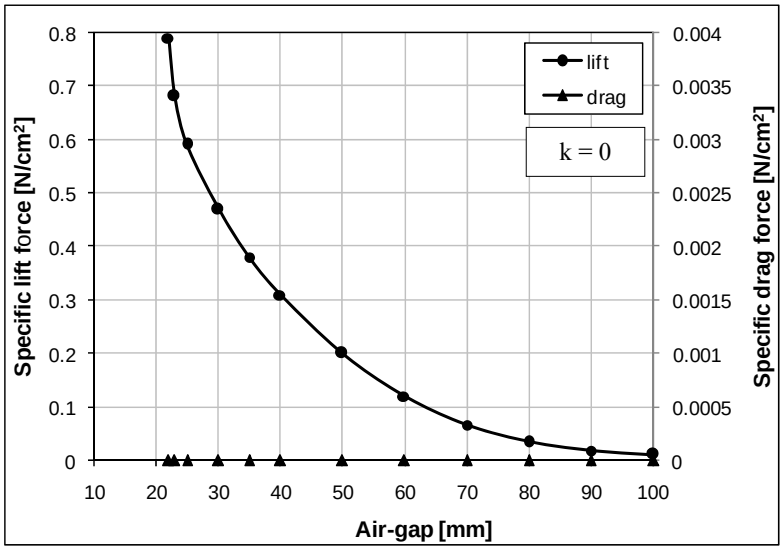

Fig. 7. Specific lift and drag force Vs. air-gap at k=0 (150 rpm).

Figs. 8 and 9 show P_Z and P_Y Vs. air-gap at 150 rpm in correspondence of perturbed (k=0.14) and strongly perturbed (k=0.33) flux configurations, respectively. Both system configurations generate drag force when the air-gap is less than 60 mm; moreover P_Z is inversely proportional to the size of the air-gap.

When the flux is strongly perturbed (k=0.33) the specific drag force is bigger than the perturbed one (k=0.14).

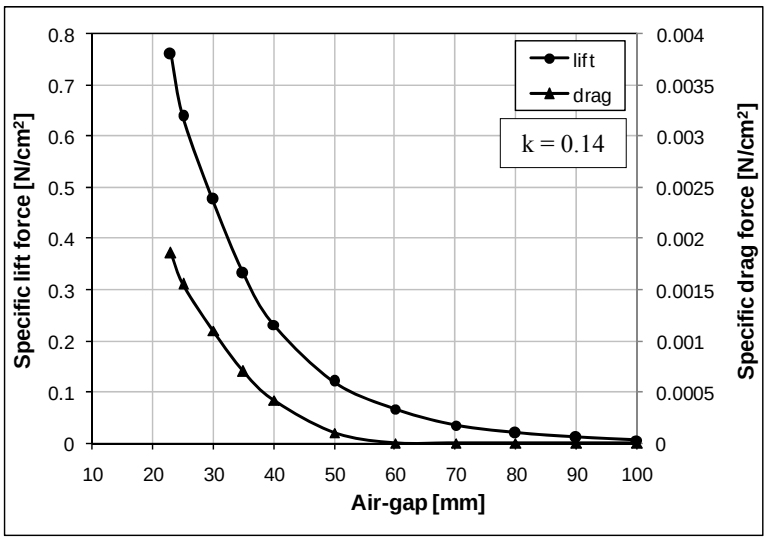

Fig. 8. Specific lift and drag force Vs. air-gap at k=0.14 (150 rpm).

It is evident that the uneven dynamic interaction between perturbed magnetic flux and HTS bulk generates on it drag force.

Comparing Figs. 8, 9 and 10, it is clear that the magnitude of drag force are directly proportional to the magnitude of the flux perturbation.

On the contrary the lift performance is not related to the magnitude of the flux perturbation.

The key lesson is that the system configuration with uniform magnetic flux (k=0) represents the best solution for HTS vehicle applications since also in the dynamic condition it produces stable lift force without drag force; on the contrary the system configurations with perturbed flux (k≠0) generate drag force when the air-gap is less than critical size (60 mm).

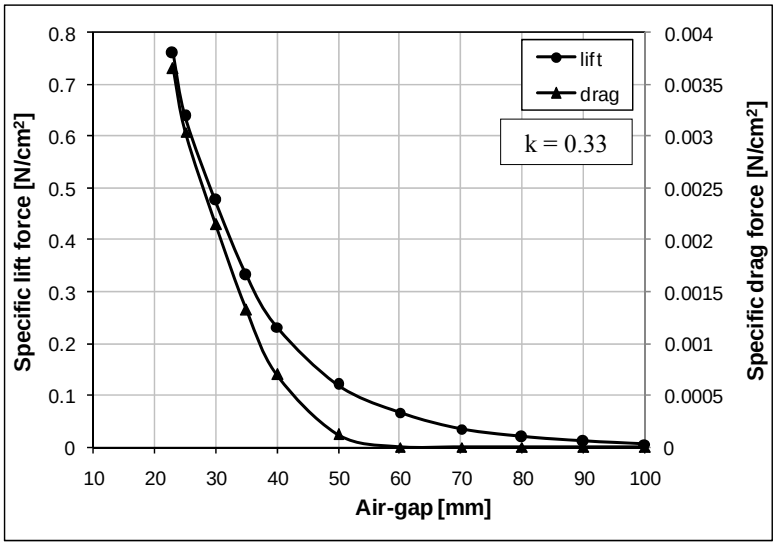

Fig. 9. Specific lift and drag force Vs. air-gap at k=0 (150 rpm).

Fig. 10 shows P_Y/P_Z in function of air-gap for the three k values. We can see that at k=0.14 and k=0.33, in correspondence of the lowest air-gap of 22 mm the specific drag force P_Y is about 0.25% and 0.48% of specific lift one P_Z.

The key lesson to be learned from these experimental results is that the drag force magnitude due to the flux perturbation is small and not comparable with lift one.

These results are very useful to gain a deeper understanding of the real behaviour of the maglev vehicle with HTS on board riding on an uneven magnetic guideway.

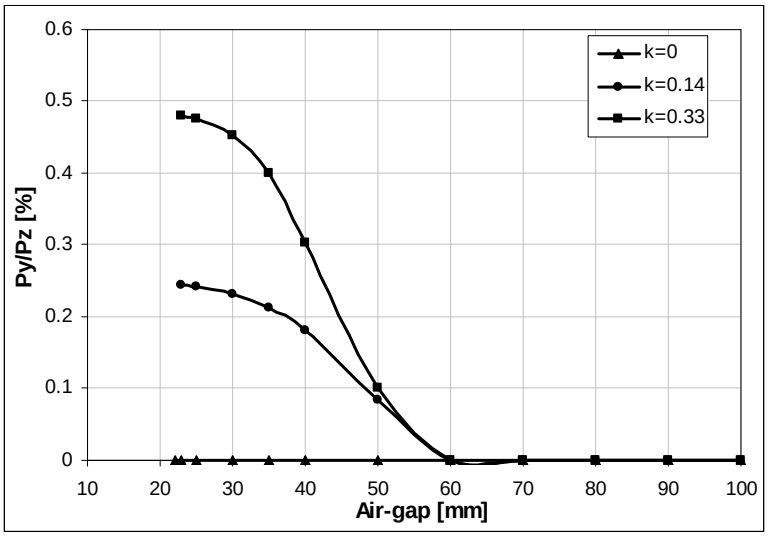

Fig. 10. P_Y/P_Z Vs. air-gap at three different values of k (150 rpm).

3. Conclusion

The influence of flux perturbation on the magneto-dynamic maglev performance of HTS bulk have been tested by means of an experimental ring model device employing the same passive YBaCuO structure interacting with a magnetic track' field differently perturbed by means of several iron plates.

The perturbation factor k is defined as total iron plates top surface and PM ring top surface ratio.

The results have shown that:

- the system configuration with uniform magnetic flux (k=0) produces stable lift force without drag force;
- systems with perturbed (k≠0) flux produce drag force when the air-gap is below 60 mm;
- the magnitude of drag force is directly proportional to the magnitude of the perturbation;
- in any case the maximum value of generated drag force is small - about 0.5% of lift force.

References

[1] Z. J. Wang, S. Wang, Y. Zeng, H. Huang, et al., Physica C, **378-381**, 809-814 (2002).
[2] Schultz et al., IEE Trans. Appl. Superconductivity **2**, 7-8 487 (1994).
[3] D'Ovidio G. Crisi F. - Navarra A. - Lanzara G., Journal of Materials Processing Technology **161**, (1-2), 45-51 (2005).
[4] D'Ovidio G. - Crisi F. - Navarra A. - Lanzara G., Journal of Physica C: Superconductivity and its applications, **449**(1), 15-20 (2006).
[5] D'Ovidio G. - Crisi F. - Navarra A. - Lanzara G, IEE Journal Transaction on Industry Application **126-D**(10), 1336-13340 (2006).

*Corresponding author: dovidio@dau.ing.univaq.it